

Supplementary information

for

**Sensitised Lanthanide Luminescence using a Ru^{II} Polypyridyl Functionalised Dipicolinic Acid
Chelate**

Divya Rajah,^a Michael C. Pfrunder,^a Bowie S. K. Chong,^a Alexander R. Ireland,^a Isaac M. Etchells, and
Evan G. Moore^{*a}

(a) School of Chemistry and Molecular Biosciences, University of Queensland, St Lucia, QLD 4072,
Australia. E-mail: egmoore@uq.edu.au

Contents

I. Experimental.....	3
II. Synthesis.....	3
III. X-ray Crystallography	6
IV. NMR Spectroscopy.	7
V. DFT/TD-DFT Calculations.....	13
VI. Photophysical Data.....	20
VII. References.....	26

I. Experimental

All reagents and solvents were purchased from commercial suppliers (Sigma Aldrich, Alfa Aesar, Precious Metals Online and Combi-Blocks) and were used without further purification. Lanthanide and Ruthenium metal salts were commercially obtained and were used in metal complexation. NMR spectra were obtained either on Bruker Avance or Ascend 500 MHz (^{13}C = 125 Hz) spectrometers and all signals were referenced with respect to the residual solvent peaks. MestReNova, Mestrelab Research software was used to process and display spectra. For mass spectrometry analyses, samples were prepared in solution using either DCM-MeOH (50:50 v/v), acetonitrile or MeOH-H₂O (60:10 v/v) at approximately 10 μM . Samples were infused at 5 μL per minute via a HESI source into an LCQ Fleet mass spectrometer in positive mode. Data was acquired across the m/z range of 200 – 2000. Source parameters included a heater temperature at sheath gas flow 5; ISV at 5 kV, ion transfer tube temperature at 275°C. Data was analysed using the on-board Xcalibur software. Elemental analyses (C, H, N) were performed by the University of Queensland School of Chemistry and Molecular Biosciences Microanalytical Service using a Thermo Scientific Flash 2000 Organic Elemental Analyser.

II. Synthesis

Dimethyl 4-hydroxypyridine-2,6-dicarboxylate (HODPAME₂)

This compound was synthesised in accordance to the literature.¹ Concentrated sulphuric acid (1 mL) was added dropwise at room temperature to a vigorously stirring suspension of chelidamic acid monohydrate (0.5 g, 2.73 mmol) in methanol (20 mL). The reaction mixture was then refluxed at 65 °C overnight. The reaction mixture was cooled to room temperature and solvent was removed in vacuo. The resulting yellow liquid was neutralised to pH 7 with saturated NaHCO₃ and extracted with dichloromethane (3 x 20 mL). The organic layer was dried over MgSO₄ and removal of the solvent in vacuo yielded a white crystalline powder (0.35 g, 61 %). ¹H NMR (500 MHz, d₄-MeOD) δ (ppm): 7.60 (s, 2H), 3.97(s, 6H). ¹³C NMR (125 MHz, d₄-MeOD) δ (ppm): 168.0, 164.7, 148.7, 115.5, 52.0. HRMS (ESI): m/z [M + H]⁺ 212.05 ; [M + Na]⁺ 234.04. Anal. Calc'd for C₉H₉NO₅ (%): C 51.19, H 4.30, N 6.63. Found C 51.22, H 4.31, N 6.40.

Dimethyl 4-bromopyridine-2,6-dicarboxylate (BrDPAME₂)

This compound was synthesised in accordance to the literature.² HODPAME₂ (1.01 g, 4.74 mmol) and phosphorus pentabromide (PBr₅) (5.07 g, 11.6 mmol) were heated at 95 °C for 3 hours. The reaction mixture was allowed to cool to room temperature and hot methanol (20 mL) was added dropwise to precipitate the desired compound. The precipitate formed was filtered and washed with minimum amount of cold methanol to afford BrDPAME₂ as beige solid (1.01 g, 77 %). ¹H NMR (500 MHz, d₄-MeOD) δ (ppm): 8.48 (s, 2H), 4.00 (s, 6H). ¹³C NMR (125 MHz, d₄-MeOD) δ (ppm): 165.2, 150.5, 136.1, 132.2, 53.6. HRMS (ESI): m/z [M + H]⁺ 273.97 ; [M + Na]⁺ 295.95. Anal. Calc'd for C₉H₈NO₄Br (%): C 39.44, H 2.94, N 5.11. Found C 39.34, H 2.90, N 5.15.

Dimethyl 4-(4,4,5,5-tetramethyl-1,3,2-dioxaborolan-2-yl)pyridine-2,6-dicarboxylate ((RO)₂B-DPAME₂)

This compound was synthesised according to the literature.³ A reaction mixture of BrDPAME₂ (0.40 g, 1.46 mmol), bis(pinacolato)diboron (0.56 g, 2.19 mmol), Pd(dppf)Cl₂ (0.02 g, 0.03 mmol), dry potassium acetate (0.43 g, 4.38 mmol) and anhydrous 1,4-dioxane (15 mL) was subjected to 3 cycles of freeze-pump-thaw, backfilled with Argon and heated at 80 °C overnight. The cooled reaction mixture was poured into water and

extracted with dichloromethane (3 x 20 mL). The organic layer was dried over MgSO₄ and yielded a pale brown solid (0.46 g, 98 %) upon removal of the solvent. ¹H NMR (500 MHz, CDCl₃) δ (ppm): 8.64 (s, 2H), 4.03 (s, 6H), 1.37 (s, 12H). ¹³C NMR (125 MHz, CDCl₃) δ (ppm): 165.2, 147.6, 133.2, 85.2, 83.5, 53.3, 25.0. HRMS (ESI): m/z [M + H]⁺ 322.15; [M + Na]⁺ 344.13. ¹H NMR analysis revealed this product was the desired compound contaminated with a small amount of unreacted bis(pinacolato)diboron, which was deemed sufficiently pure to use in the next step without further purification.

Complexation of [(tpy)RuCl₃]³⁺

This complex was synthesised following a literature method.⁴ A solution of 2,2':6',2''-terpyridine (tpy) (0.40 g, 1.71 mmol) dissolved in ethanol (50 mL) was added dropwise to [RuCl₃(H₂O)₃] (0.51 g, 1.95 mmol) dissolved in ethanol (50 mL). The reaction mixture was stirred and heated to reflux under Argon for 3 hours. Upon cooling to room temperature, the precipitate obtained was filtered and washed with cold ethanol followed with diethyl ether to afford a black solid (0.72 g, 1.63 mmol). Anal. Calc'd for RuC₁₅N₃H₁₁Cl₃·0.25H₂O (%): C 40.47, H 2.60, N 9.44. Found C 40.27, H 2.46, N 9.42. [(tpy)RuCl₃]³⁺ was used in the next step without further purification.

[(tpy)Ru^{II}(tpyPh-Br)](PF₆)₂

This complex was prepared according to modified literature procedures.⁴⁻⁶ Briefly, [(tpy)Ru^{III}Cl₃] (0.39 g, 0.88 mmol) and silver tetrafluoroborate (0.52 g, 2.65 mmol) dissolved in a mixture of 4:1 acetone (90 mL) and ethanol (22.5 mL) was heated to reflux for 3 hours. The reaction mixture was cooled to room temperature and the precipitated silver chloride (AgCl) was removed by filtration. Ethanol (20 mL) was added to the filtrate and the acetone was removed in vacuo. The residual of the filtrate was dissolved in acetone and added dropwise to a reaction mixture of 4'-(4-bromophenyl)-2,2':6',2''-terpyridine (tpyPh-Br) (0.35 g, 0.90 mmol) dissolved in ethanol (30 mL) and 4-ethylmorpholine (1 mL). The dark purple reaction mixture was heated to reflux at 70 °C under Argon for 3 hours which resulted in a maroon solution. Upon cooling to room temperature, an aqueous solution of saturated KPF₆ (1 mL) was added to the reaction mixture and the solvent was removed under reduced pressure. The crude mixture was passed through an alumina plug using MeCN. The red band was collected and further purified via silica column using a solvent mixture of 90:7:3 (MeCN: H₂O: sat. KNO₃(aq)). The second fraction was collected, and solvent was removed to yield the desired complex. [(tpy)Ru^{II}(tpyPh-Br)](PF₆)₂ was precipitated by adding a saturated aqueous solution of KPF₆ (3 mL) yielding (0.39 g, 61 %). ¹H NMR (500 MHz, CD₃CN) δ (ppm): 9.00 (s, 2H), 8.77 (d, J = 8.2 Hz, 2H), 8.65 (d, J = 8.0 Hz, 2H), 8.51 (d, J = 8.1 Hz, 2H), 8.42 (t, J = 8.2 Hz, 1H), 8.13 (d, J = 8.5 Hz, 1H), 7.99 – 7.89 (m, 6H), 7.41 (d, J = 5.3 Hz, 2H), 7.36 (d, J = 5.2 Hz, 2H), 7.17 – 7.14 (m, 4H). HRMS (ESI): m/z [M]²⁺ 362.02. Anal. Calc'd for [Ru(C₁₅H₁₁N₃)(C₂₁H₁₄N₃Br)](PF₆)₂·H₂O (%): C 41.96, H 2.64, N 8.15. Found C 41.80, H 2.41, N 7.86.

[(tpy)Ru^{II}(tpyPh-DPAMe₂)](PF₆)₂

This complex was synthesised according to modified literature methods.^{4, 7} A solution of [(tpy)Ru^{II}(tpyPh-Br)](PF₆)₂ (0.10 g, 0.10 mmol), (RO)₂B-DPAMe₂, (0.04 g, 0.13 mmol) and potassium carbonate (0.52 g, 0.37 mmol) in DMSO (5 mL) was subjected to 3 cycles of freeze-pump-thaw. Pd(PPh₃)₂Cl₂ (0.01 g, 0.01 mmol) was added to the reaction mixture under Argon which was subjected to another cycle of freeze-pump-thaw. The reaction mixture was heated to reflux at 75 °C under argon for 24 hours. Upon cooling to room temperature, saturated KPF₆ and water were added to the reaction mixture. The precipitate formed was filtered and washed with water. The crude mixture was purified via silica column using a solvent mixture of 90:7:3 (MeCN: H₂O: sat. KNO₃(aq)). The first band eluted was collected and the solvent was removed to yield the desired compound. [(tpy)Ru^{II}(tpyPh-DPAMe₂)](PF₆)₂ was precipitated by adding an aqueous solution of saturated KPF₆

(3 mL) yielding (0.03 g, 10 %). ^1H NMR (500 MHz, CD_3CN) δ (ppm): 9.08 (s, 2H), 8.78 (d, $J = 8.2$ Hz, 2H), 8.73 – 8.68 (m, 4H), 8.53 (d, $J = 7.9$ Hz, 2H), 8.47 – 8.37 (m, 3H), 8.23 (d, $J = 8.2$ Hz, 2H), 7.95 (dtd, $J = 15.7, 7.8, 1.5$ Hz, 4H), 7.47 (d, $J = 5.3$ Hz, 1H), 7.37 (d, $J = 5.7$ Hz, 4H), 7.22 – 7.15 (m, 4H). HRMS (ESI): m/z $[\text{M}]^{2+}$ 418.58. Calc'd for $[(\text{Ru}(\text{C}_{15}\text{H}_{11}\text{N}_3)(\text{C}_{30}\text{H}_{22}\text{N}_4\text{O}_4))(\text{PF}_6)_2]\cdot\text{KPF}_6$ (%): C 44.35, H 2.73, N 8.04. Found C 44.17, H 2.71, N 7.80.

$[(\text{tpy})\text{Ru}^{\text{II}}(\text{tpyPh-DPA})](\text{PF}_6)_2$

A solution of KOH dissolved in 6:1 (v/v) MeCN: H_2O was added dropwise to $[(\text{tpy})\text{Ru}^{\text{II}}(\text{tpyPh-DPAME}_2)](\text{PF}_6)_2$ (0.03g, 0.02 mmol) in 6:1 (v/v) MeCN: H_2O until a red precipitate was formed. The precipitate was centrifuged with the solvent mixture followed by MeCN. The supernatant was decanted, and the precipitate was dissolved in distilled H_2O . Concentrated HPF_6 was added until a red precipitate of $[(\text{tpy})\text{Ru}^{\text{II}}(\text{tpyPh-DPA})]$ was formed (0.02 g, 53 %). ^1H NMR (500 MHz, 2:1 d_4 -MeOD: D_2O v/v) δ (ppm): 9.26 (s, 2H), 8.91 (d, $J = 8.2$ Hz, 2H), 8.82 (d, $J = 8.2$ Hz, 2H), 8.66 (d, $J = 8.1$ Hz, 2H), 8.57 (s, 2H), 8.54 – 8.42 (m, 3H), 8.25 (d, $J = 8.1$ Hz, 2H), 8.10 – 7.96 (m, 4H), 7.49 (d, $J = 5.6$ Hz, 2H), 7.43 (d, $J = 5.6$ Hz, 2H), 7.28 (q, $J = 4.9, 2.8$ Hz, 4H). HRMS (ESI): m/z $[\text{M}]^{2+}$ 404.57. Calc'd for $[\text{Ru}(\text{C}_{15}\text{H}_{11}\text{N}_3)(\text{C}_{28}\text{H}_{16}\text{N}_4\text{O}_4)](\text{PF}_6)_2\cdot\text{HPF}_6$ (%): C 41.49, H 2.43, N 7.88. Found C 42.05, H 2.64, N 7.67.

$[(\text{tpy})\text{Ru}^{\text{II}}(\text{tpyPh-DPA})\text{Ln}^{\text{III}}(\text{H}_2\text{O})_x]^{3+}$ ($\text{Ln}^{\text{III}} = \text{Lu}^{\text{III}}, \text{Yb}^{\text{III}}, \text{Er}^{\text{III}}$ and Nd^{III})

General method for formation of Ln^{III} complexes

An aqueous solution of MES buffer (25 mL, 0.7 M) (MES = 2-(N-morpholino)ethanesulfonic acid) was prepared and adjusted to pH 6 using aqueous KOH (ca. 1 M).

A 1.43 mL portion of this buffer was evaporated to dryness over high vacuum and was subsequently reconstituted 3.33 mL of D_2O , which was then diluted with d_4 -MeOD to a final volume of 10 mL (2:1 d_4 -MeOD: D_2O v/v, 0.1 M, $\text{pD} \approx 6.4$)⁸

This solution was then used to prepare a stock solution of $[(\text{tpy})\text{Ru}^{\text{II}}(\text{tpyPh-DPA})]$ (0.8 mg/mL) which was used for subsequent photophysical characterisation and in situ $\text{Ln}(\text{III})$ complex formation.

To prepare the required $\text{Ln}(\text{III})$ complexes, an excess (10 mg) of $[\text{Ln}(\text{OTf})_3\cdot x\text{H}_2\text{O}]$ salt was added to a portion (700 μL) of the stock solution of $[(\text{tpy})\text{Ru}^{\text{II}}(\text{tpyPh-DPA})]$. The formation of the desired 1:1 complexes was evidenced by HRMS analysis of the $\text{Lu}(\text{III})$ complex, and for the $\text{Lu}(\text{III})$ and $\text{Nd}(\text{III})$ complexes, successful complexation was also confirmed by ^1H NMR.

$\text{Lu}(\text{III})$ complex: ^1H NMR (500 MHz, 2:1 d_4 -MeOD: D_2O v/v) δ (ppm): 9.28 (s, 2H), 8.93 (d, $J = 8.2$ Hz, 2H), 8.84 (d, $J = 8.2$ Hz, 2H), 8.67 (d, $J = 8.1$ Hz, 2H), 8.63 (s, 2H), 8.52 (dd, $J = 8.2, 5.6$ Hz, 3H), 8.31 (d, $J = 8.0$ Hz, 2H), 8.11 – 7.96 (m, 4H), 7.47 (dd, $J = 24.3, 5.6$ Hz, 4H), 7.30 (q, $J = 6.4$ Hz, 4H).

HRMS (ESI): m/z $[(\text{tpy})\text{Ru}^{\text{II}}(\text{tpyPh-DPA})\text{Lu}(\text{H}_2\text{O})_4]^{3+}$ 351.37, $[(\text{tpy})\text{Ru}^{\text{II}}(\text{tpyPh-DPA})\text{Lu}(\text{H}_2\text{O})(\text{MeOH})_2]^{3+}$ 354.71, $[(\text{tpy})\text{Ru}^{\text{II}}(\text{tpyPh-DPA})\text{Lu}(\text{H}_2\text{O})_5]^{3+}$ 357.37, $[(\text{tpy})\text{Ru}^{\text{II}}(\text{tpyPh-DPA})\text{Lu}(\text{H}_2\text{O})_2(\text{MeOH})_2]^{3+}$ 360.71.

$\text{Nd}(\text{III})$ complex: ^1H NMR (500 MHz, 2:1 d_4 -MeOD: D_2O v/v) δ (ppm): 12.00 (s, 2H), 9.55 (s, 2H), 9.42 (d, $J = 7.6$ Hz, 2H), 8.98 (dd, $J = 15.1, 8.2$ Hz, 4H), 8.91 (d, $J = 7.4$ Hz, 2H), 8.71 (d, $J = 8.1$ Hz, 1H), 8.58 – 8.51 (m, 1H), 8.14 (t, $J = 7.7$ Hz, 2H), 8.06 (t, $J = 7.7$ Hz, 2H), 7.62 (d, $J = 5.7$ Hz, 2H), 7.51 (d, $J = 5.6$ Hz, 2H), 7.40 – 7.33 (m, 4H).

III. X-ray Crystallography

Data for [(tpy)Ru^{II}(tpyPh-DPAMe₂)](PF₆)₂ were collected at at 100 K on a Rigaku Synergy diffractometer using Mo K α radiation ($\lambda = 0.71073$) from a sealed tube operating at 50 kV and 1mA. Data reduction, integration and empirical absorption correction (ψ -scans) were performed within the CrysAlisPro⁹ software package, with subsequent computations carried out using OLEX-2.¹⁰The structure solution was obtained using SHELXT¹¹ and a full matrix least-squares refinement was carried out with SHELXL¹² through the OLEX-2 interface. Reflections at angles greater than 50° 2θ were omitted, and non-H atoms were refined using anisotropic displacement parameters. Diffraction was less than ideal being both broad and weak and with very few reflections observed at above 0.9 Å resolution which resulted in larger than expected residuals, however the data proved sufficient to unambiguously confirm the atomic connectivity of the primary residue. The structure was found to be a 2-fold twin with a 180° rotation about the [-105] direct lattice direction. Disordered PF₆⁻ ion containing phosphorus P3 was modelled as a rigid body with anisotropic displacement parameters as a suitable second position could not be located in the difference Fourier map. The remaining PF₆⁻ ions were each modelled over two positions with the aid of atomic distance restraints (DFIX). A global restraint was placed on the relationship between the vectors of neighbouring non-hydrogen atoms (RIGU) to prevent non-positive definites, and, where necessary, thermal parameters were further restrained to approximate isotropic displacement (ISOR). The CIF file has been deposited with the CSD (CCDC # 2065117). Crystal data for [(tpy)Ru^{II}(tpyPh-DPA)](PF₆)₂ (M= 1310.86 g mol⁻¹): Formula C₄₅H₃₃F₁₈KN₇O₄P₃Ru, triclinic, space group $P\bar{1}$, a = 9.1630(5) Å, b = 11.2045(6) Å, c = 24.0190(18) Å, $\alpha = 89.234(5)^\circ$, $\beta = 85.686(5)^\circ$, $\gamma = 79.545(5)^\circ$, V = 2418.2(3) Å³, Z = 2, crystal dimensions 0.14 × 0.11 × 0.01 mm, colour orange, habit plate, T= 100(2) K, $\mu(\text{MoK}\alpha) = 0.633 \text{ mm}^{-1}$, $D_{\text{calc}} = 1.800 \text{ g cm}^{-3}$, $T_{\text{mix,max}} = 0.40176, 1.00000, 21\ 954$ reflections measured (hkl range -10 10, -12 13, -28 25), 8324 unique ($R_{\text{int}} = 0.0914$) which were used in all calculations. The final R_1 was 0.1280 ($I > 2\sigma(I)$)*, wR_2 was 0.3709 (all data)* and GoF on F₂ was 1.069 (all data), $Dr_{\text{min,max}} = -1.545, 2.912 \text{ e}^{-\text{Å}^{-3}}$. * $R_1 = \sum ||F_o| - |F_c|| / \sum |F_o|$ for $F_o > 2\sigma(F_o)$; $wR_2 = (\sum w(F_o^2 - F_c^2)^2 / \sum (wF_c^2)^2)^{1/2}$ all reflections.

IV. NMR Spectroscopy.

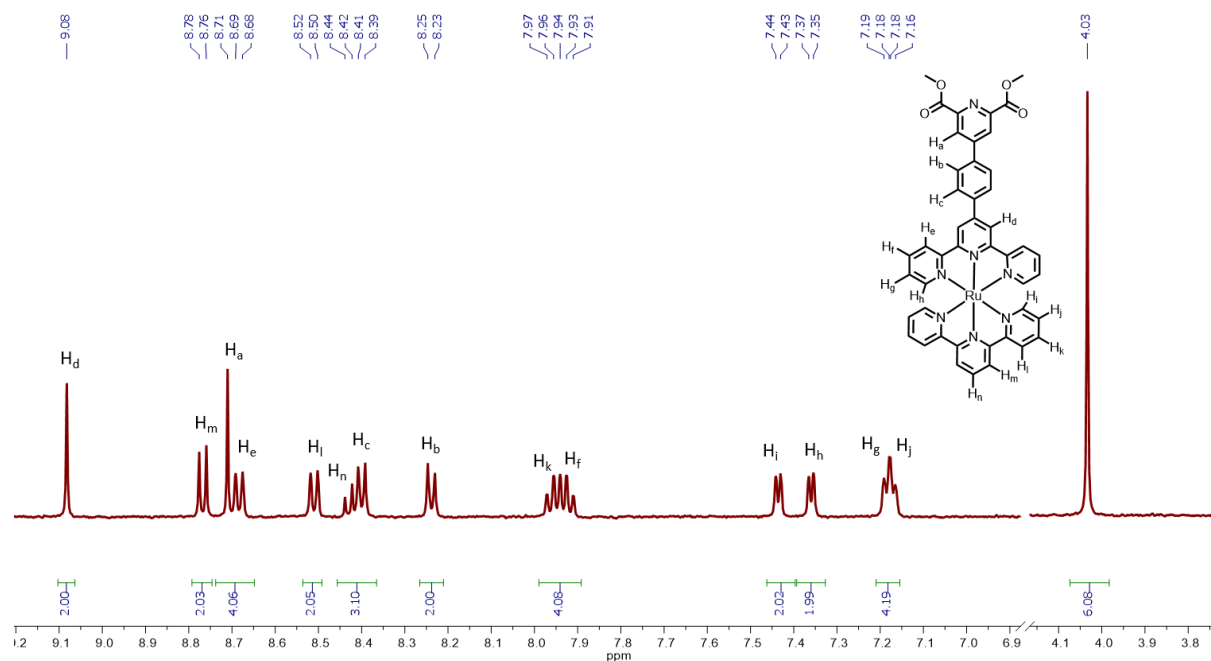


Figure S1: Assigned ^1H NMR spectrum of $[(\text{tpy})\text{Ru}^{\text{II}}(\text{tpyPh-DPAME}_2)]^{2+}$ in CD_3CN , 500 MHz.

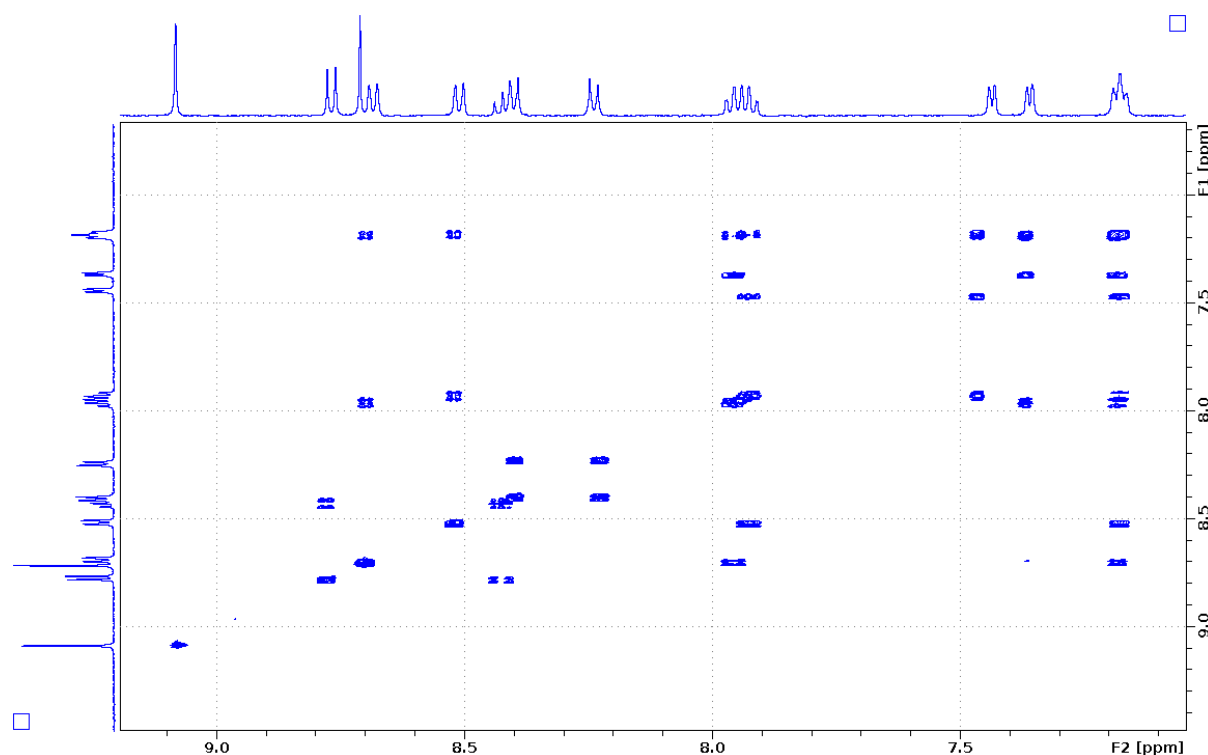


Figure S2: ^1H - ^1H COSY NMR spectrum of $[(\text{tpy})\text{Ru}^{\text{II}}(\text{tpyPh-DPAME}_2)]^{2+}$ in CD_3CN , 500 MHz

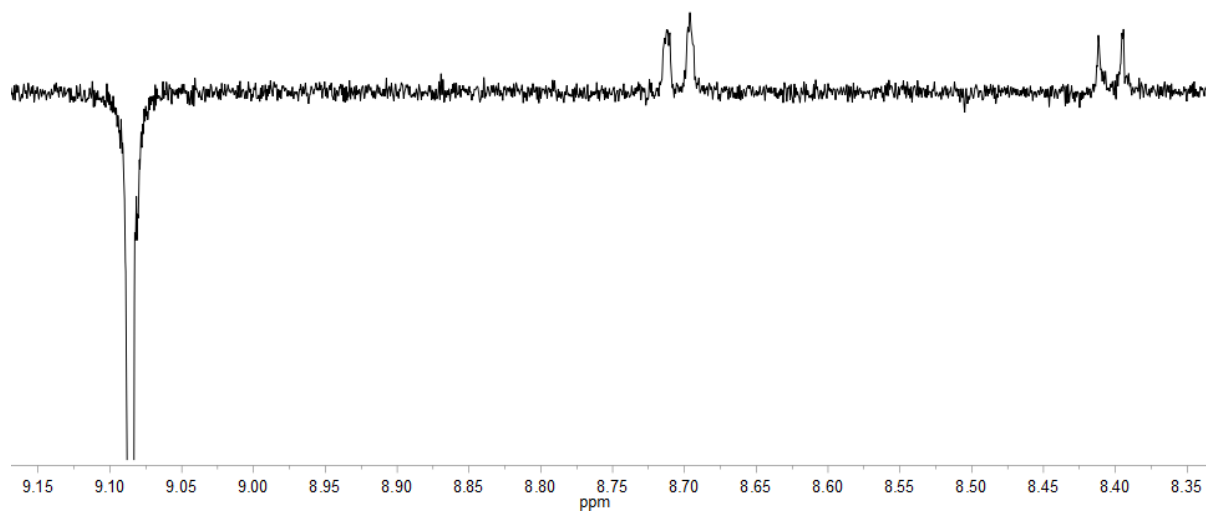


Figure S3: 1D-NOESY spectrum of $[(\text{tpy})\text{Ru}^{\text{II}}(\text{tpyPh-DPAMe}_2)]^{2+}$ irradiating at 9.08 ppm CD_3CN , 500 MHz.

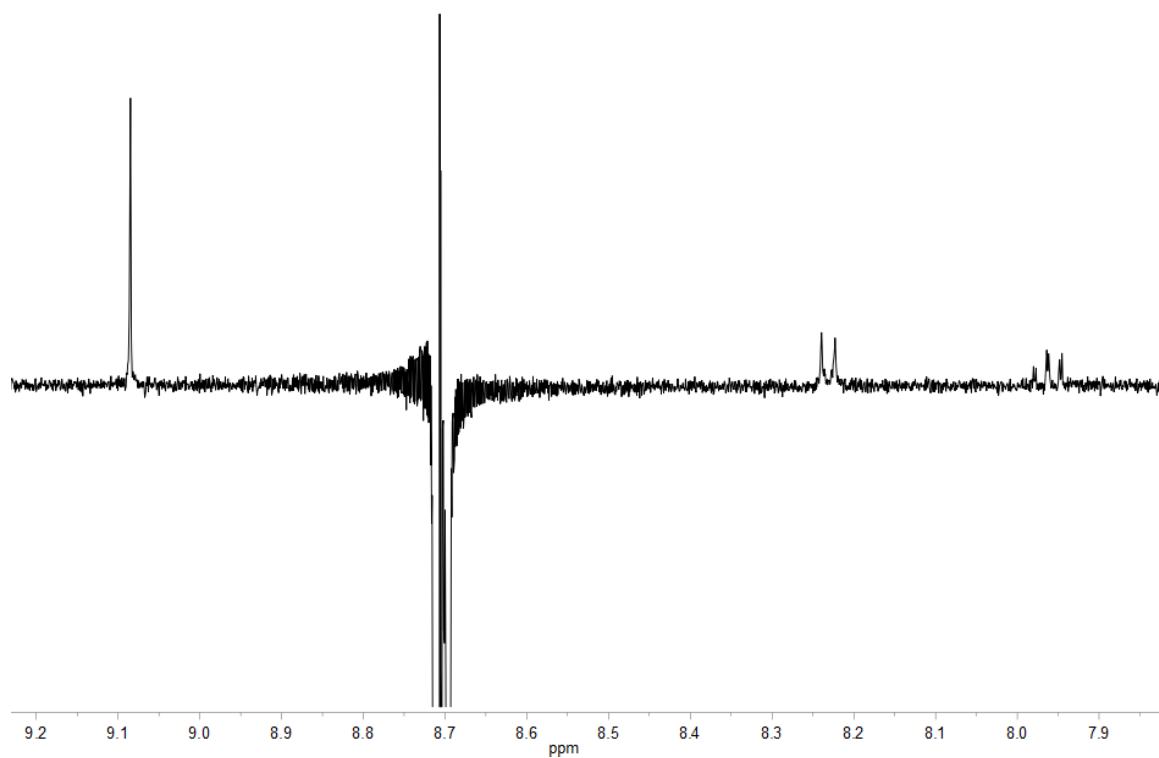


Figure S4: 1D-NOESY spectrum of $[(\text{tpy})\text{Ru}^{\text{II}}(\text{tpyPh-DPAMe}_2)]^{2+}$ irradiating at 8.71 ppm CD_3CN , 500 MHz.

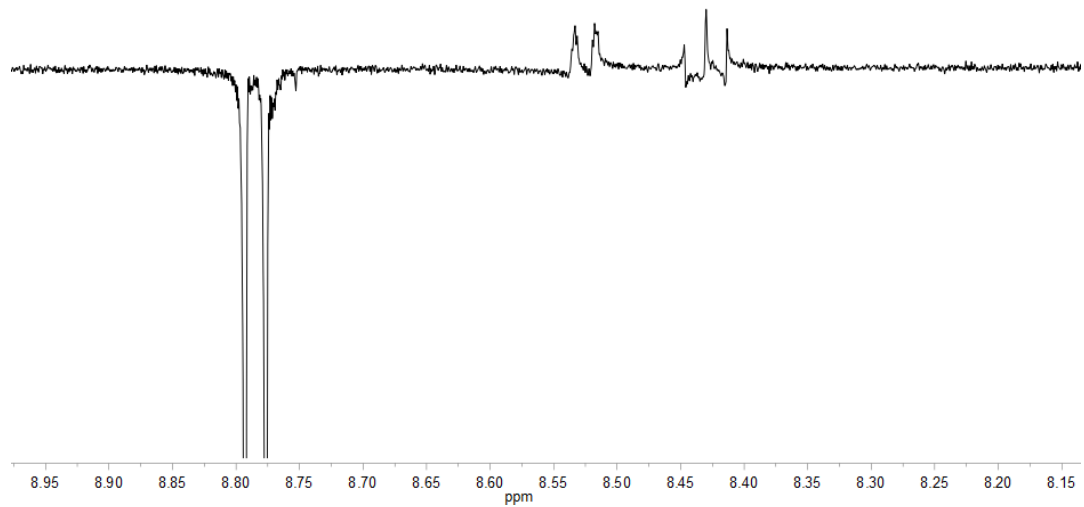


Figure S5: 1D-NOESY spectrum of $[(\text{tpy})\text{Ru}^{\text{II}}(\text{tpyPh-DPAMe}_2)]^{2+}$ irradiating at 8.78 ppm CD_3CN , 500 MHz.

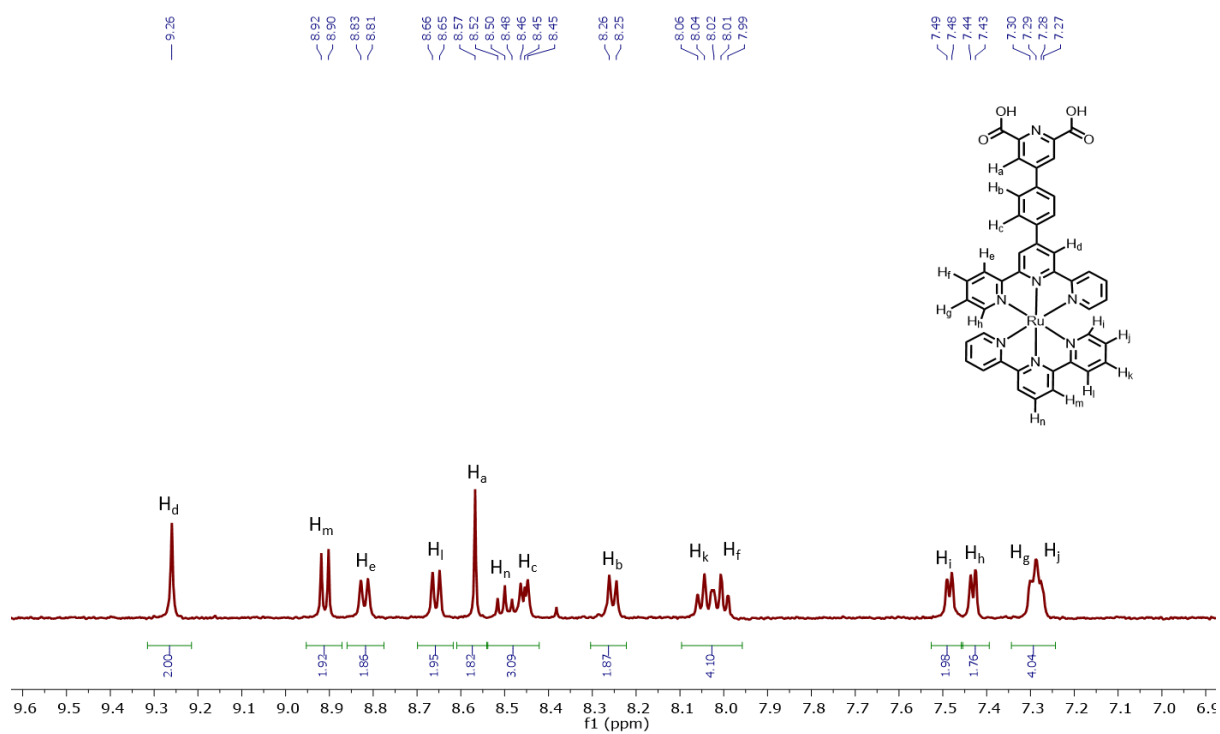


Figure S6: Assigned ^1H NMR spectrum of $[(\text{tpy})\text{Ru}^{\text{II}}(\text{tpyPh-DPA})]^{2+}$ in 2:1 $\text{d}_4\text{-MeOD}:\text{D}_2\text{O}$ v/v, 500 MHz.

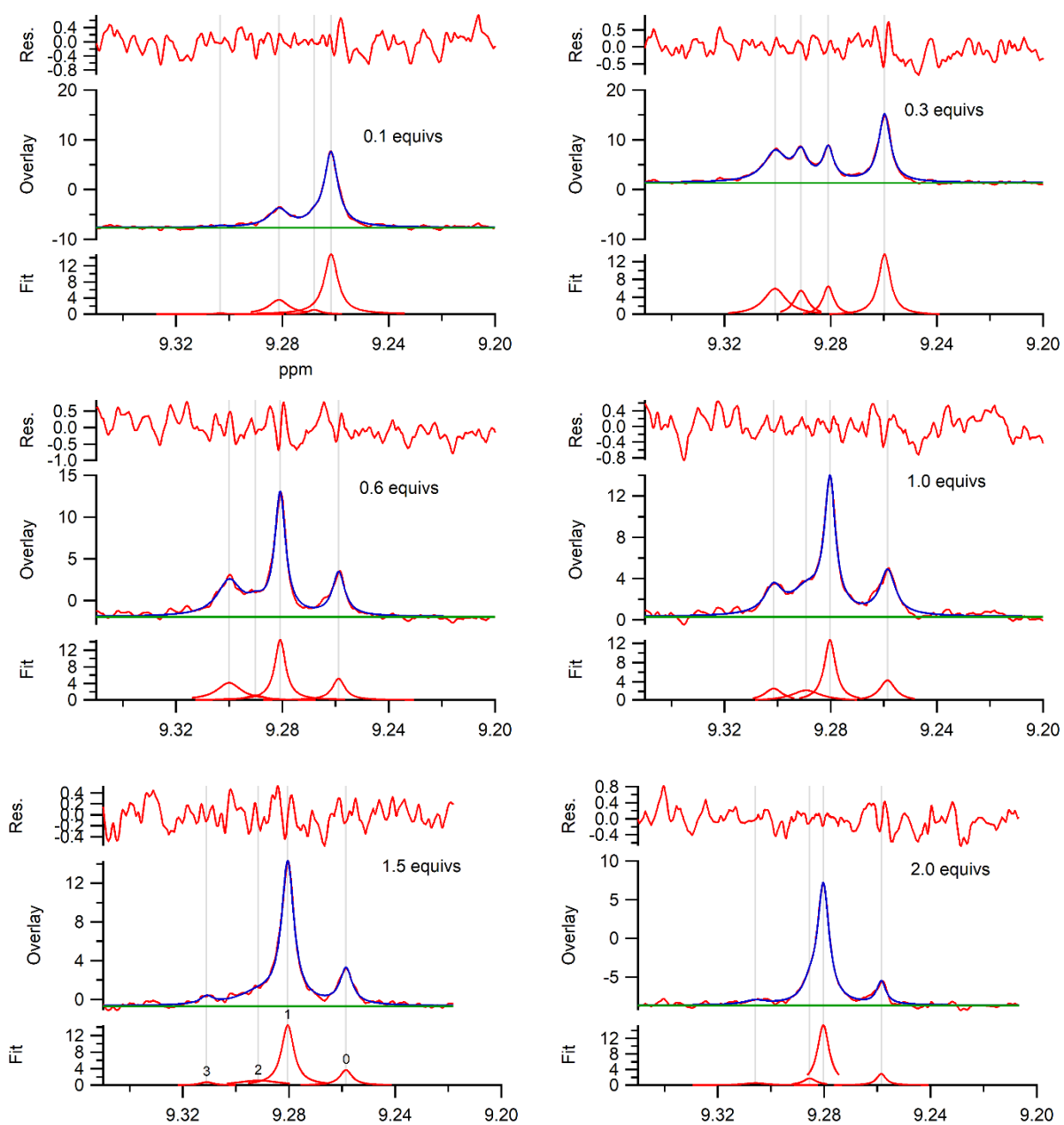


Figure S7: ^1H NMR data showing fitting of curves to H_d of respective $(\text{ML})_x\text{Lu}^{\text{III}}$ species for successive concentrations of $\text{Lu}(\text{OTf})_3 \cdot 6\text{H}_2\text{O}$. Theoretical fit (bottom), theoretical fit overlaid with experimental data (middle) and residuals to fit (top).

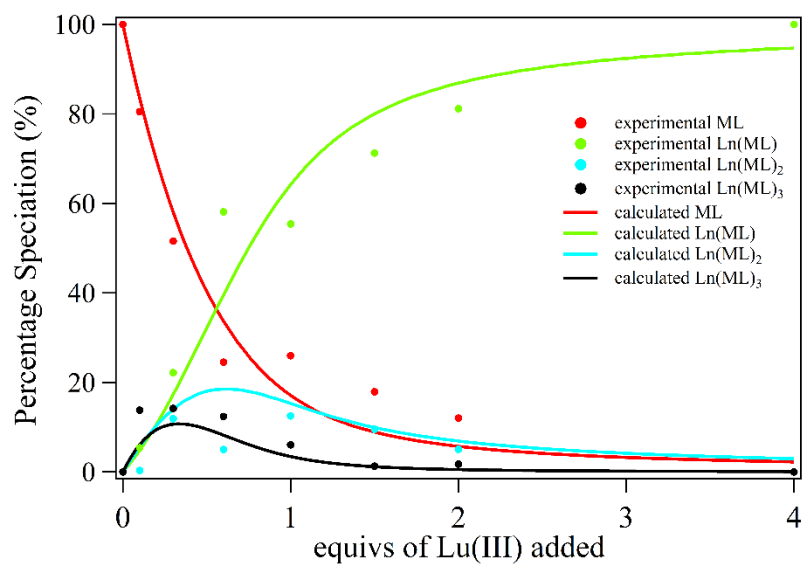


Figure S8: The experimental and calculated speciation diagram of $[(\text{tpy})\text{Ru}^{\text{II}}(\text{tpyPh-DPA})\text{Lu}^{\text{III}}(\text{H}_2\text{O})_x]^{3+}$ with varying concentrations of $\text{Lu}(\text{OTf})_3 \cdot 6\text{H}_2\text{O}$. Relative concentrations of each species were calculated by fitting a series of Lorentzian functions to the ^1H NMR signals of H_d for each species (accounting for ^1H signal multiplicity) as shown in Figure S7.

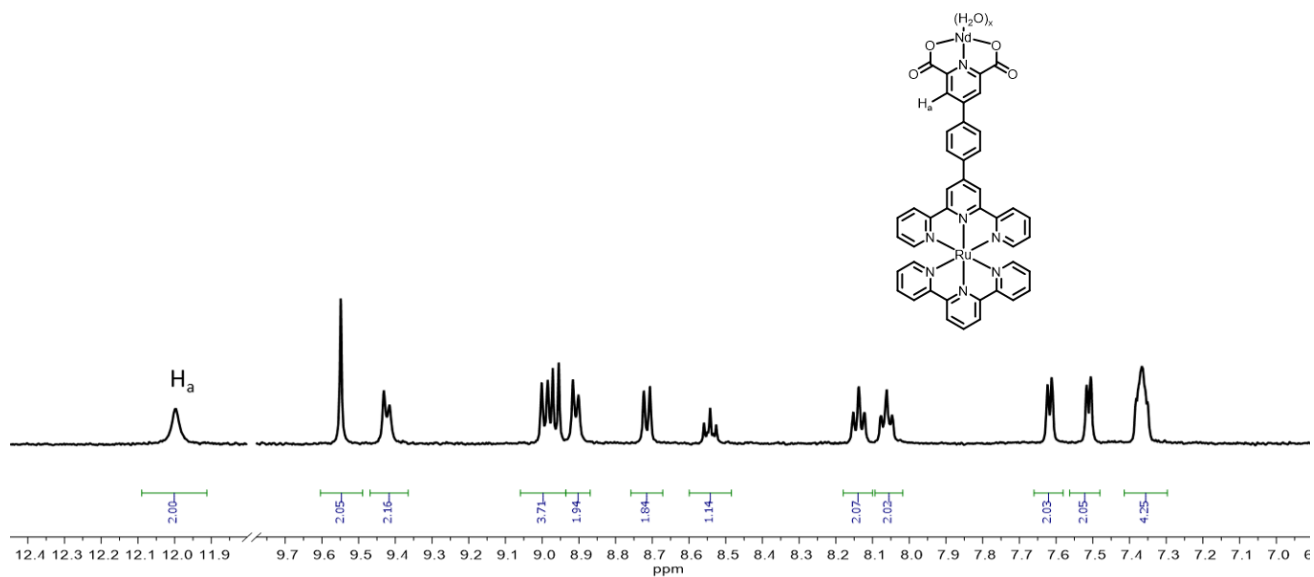


Figure S9 NMR spectrum of $[(\text{tpy})\text{Ru}^{\text{II}}(\text{tpyPh-DPA})\text{Nd}^{\text{III}}(\text{H}_2\text{O})_x]^{3+}$ prepared by addition of $\text{Nd}(\text{OTf})_3 \cdot 6\text{H}_2\text{O}$ (10 mg) to a solution of $[(\text{tpy})\text{Ru}^{\text{II}}(\text{tpyPh-DPA})]^{2+}$ (0.8 mg/mL) in (2:1 $\text{d}_4\text{-MeOD}:\text{D}_2\text{O}$ v/v) with deuterated MES buffer (0.1M, pD 6.4).

V. DFT/TD-DFT Calculations

Density Functional Theory (DFT) calculations were performed using the Gaussian 16 package (Revision B.01).¹³ Ground state geometry optimisations of $[(\text{tpy})\text{Ru}^{\text{II}}(\text{tpyPh-DPA})]^{2+}$ and $[(\text{tpy})\text{Ru}^{\text{II}}(\text{tpyPh-DPA})\text{Lu}^{\text{III}}(\text{H}_2\text{O})_x]^{3+}$ were conducted using mPW1PW91 functional¹⁴ with the D95V basis set¹⁵ for C, H, N, O atoms, the LanL2TZ(f) basis set¹⁶⁻¹⁸ for the Ru atom and the def2-QZVP basis set^{18,19} for the Lu^{III} ion, together with the SMD implicit solvent model²⁰ to simulate the solvent (methanol). The ultrafine integration grid of Gaussian 16 was used. Subsequent frequency calculations of the optimized structures were performed to ensure no imaginary vibrational frequencies were present. Corresponding calculations of the singlet and triplet excited state energies were undertaken using Time-Dependent (TD-DFT) methods in Gaussian 16, using the same functional and basis sets. A summary of the results is presented in Fig 3., Table S1 and Figure S12 – S14.

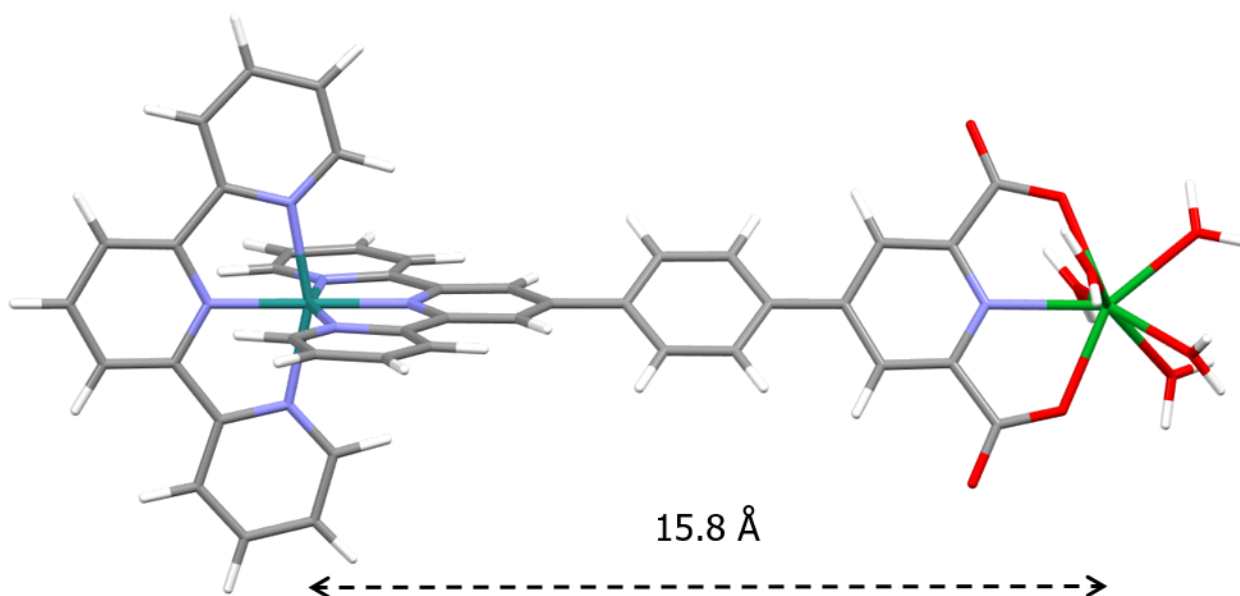


Figure S10. DFT optimised structure of $[(\text{tpy})\text{Ru}^{\text{II}}(\text{tpyPh-DPA})\text{Lu}^{\text{III}}(\text{H}_2\text{O})_5]^{3+}$ showing intra-metallic distance.

Table S1. Summary of the results of the lowest excited states calculation from TD-DFT, MPW1PW91/D95V/LanL2TZ(f) (Ru^{II})/def2-QZVP (Lu^{III})/SMD:methanol.

[(tpy)Ru^{II}(tpyPh-DPA)]³⁺				
Excited State	Singlet	2.4677 eV	502.43 nm	f = 0.0165
191 → 192	0.69429	HOMO → LUMO	96.4 %	TPY_Ph_DPA_MLCT
Excited State	Triplet	1.9962 eV	621.11 nm	f = 0.0000
189 → 193	-0.19339	HOMO -2 → LUMO +1	7.5 %	TPY MLCT
190 → 192	0.64664	HOMO -1 → LUMO	83.7 %	TPY_Ph_DPA MLCT
[(tpy)Ru^{II}(tpyPh-DPA)Lu^{III}(H₂O)₅]³⁺				
Excited State	Singlet	2.4677 eV	502.43 nm	f = 0.0165
236 → 237	0.63802	HOMO → LUMO	81.4 %	TPY_Ph_DPA MLCT
236 → 240	0.2887	HOMO → LUMO +3	16.7 %	TPY_Ph_DPA_MLCT
Excited State	Triplet	1.9876 eV	623.78 nm	f = 0.0000
234 → 238	-0.16699	HOMO -2 → LUMO +1	5.6 %	TPY MLCT
235 → 237	0.60604	HOMO -1 → LUMO	73.5 %	TPY_Ph_DPA MLCT
235 → 240	0.25826	HOMO -1 → LUMO +3	13.3 %	TPY_Ph_DPA MLCT

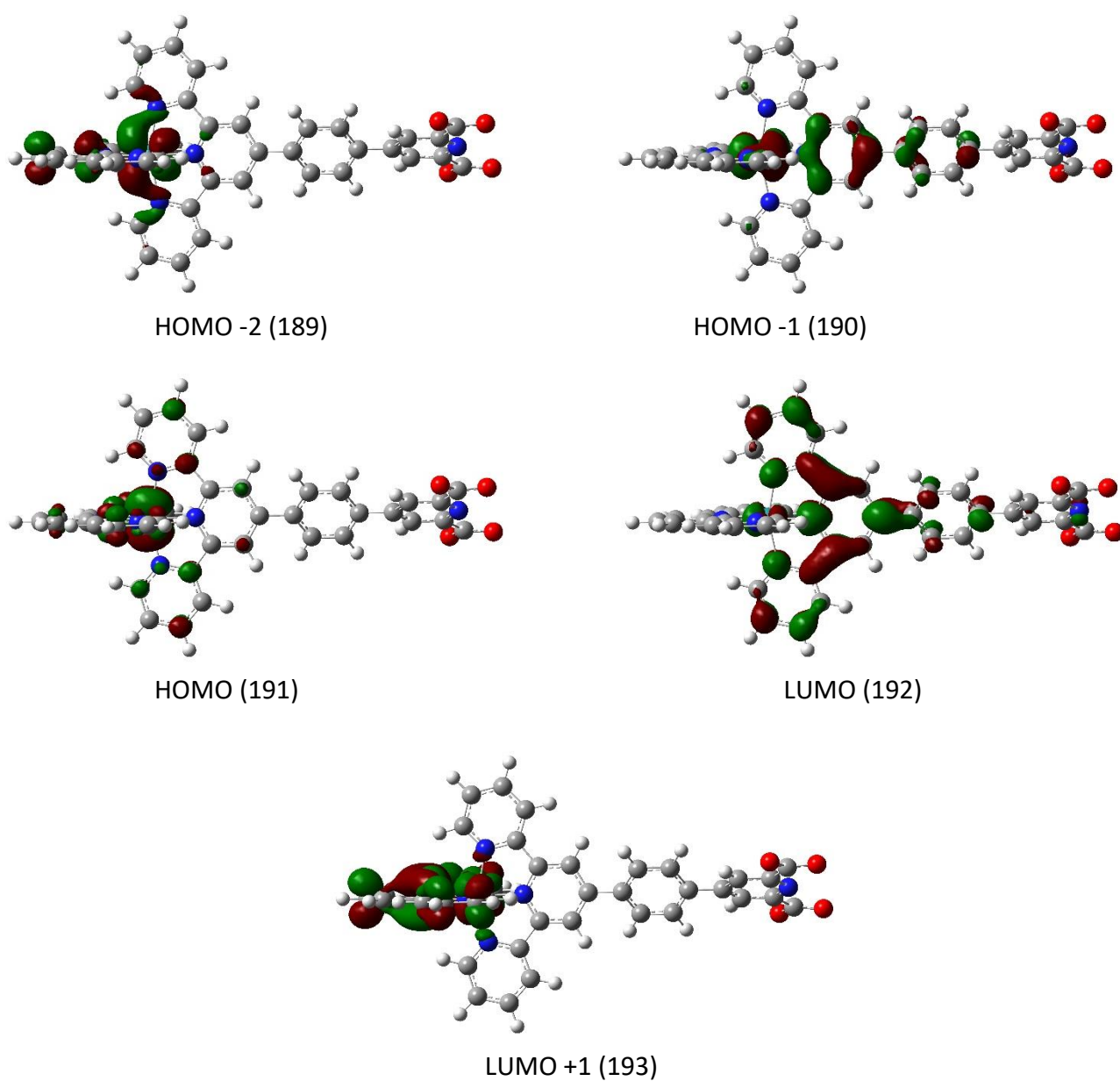


Figure S11. TD-DFT molecular orbitals of the excited state of [(tpy)Ru^{II}(tpyPh-DPA)] metalloligand with mPW1PW91/D95V/LanL2TZ(f) (Ru^{II})/SMD: Methanol.

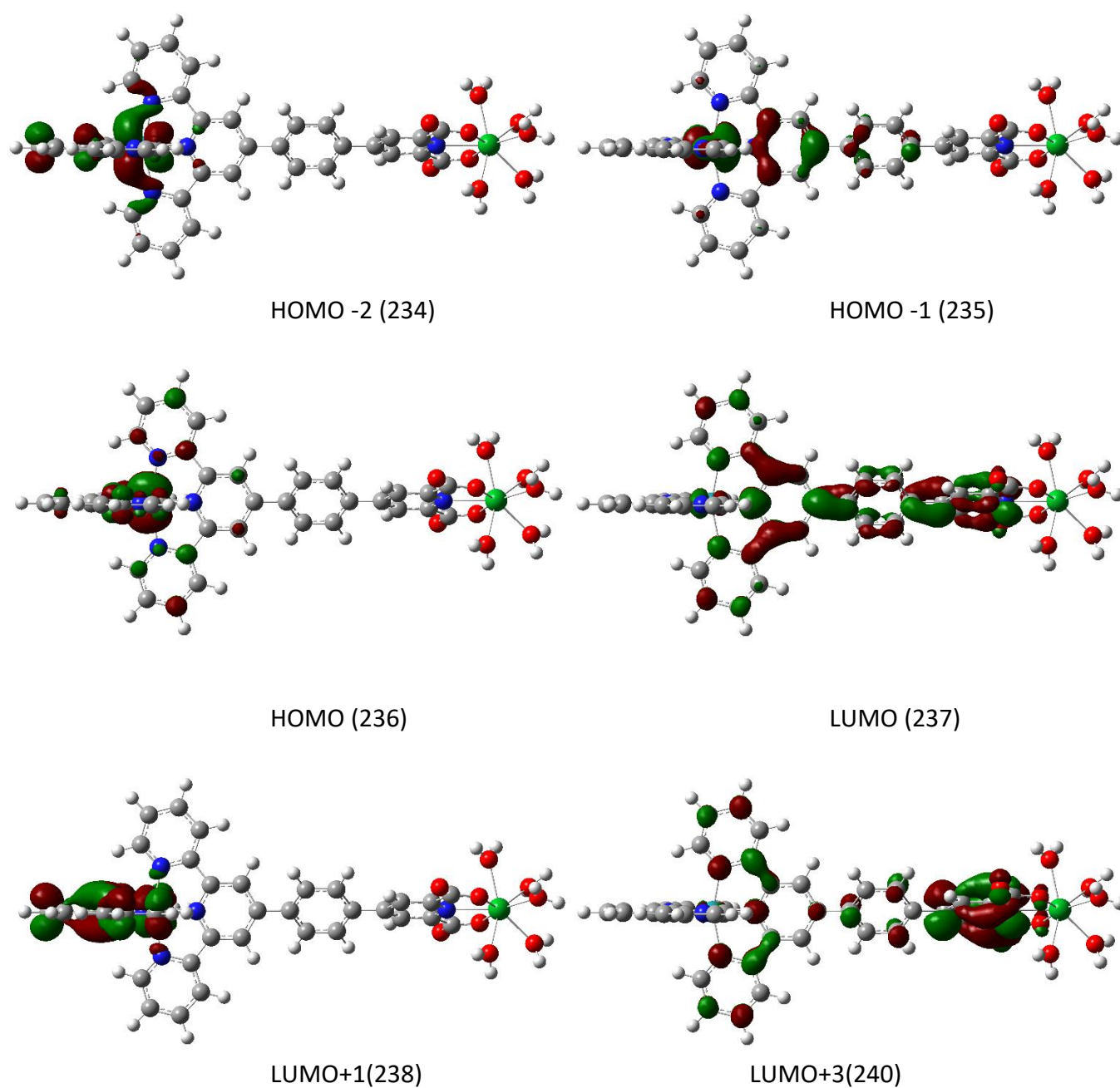


Figure S12. TD-DFT molecular orbitals of the excited state of $[(\text{tpy})\text{Ru}^{\text{II}}(\text{tpyPh-DPA})\text{Lu}^{\text{III}}(\text{H}_2\text{O})_5]^{3+}$ with mPW1PW91/D95V/LanL2TZ(f) (Ru^{II})/SMD:Methanol.

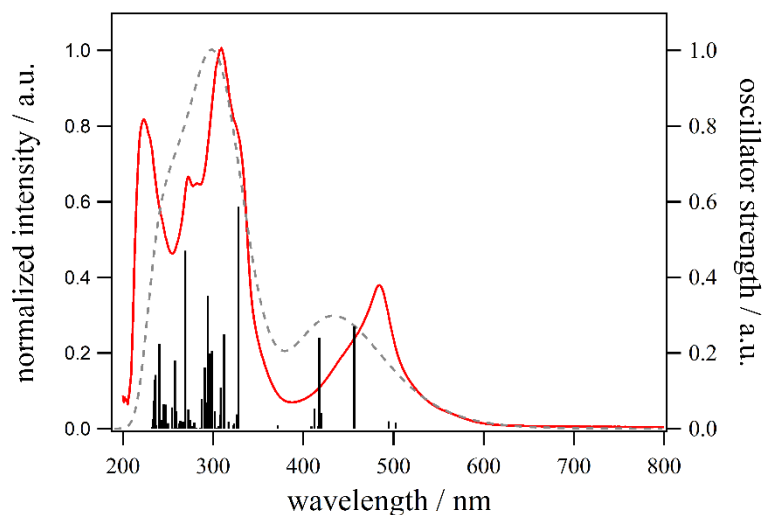


Figure S13. Comparison of UV-Vis absorption spectrum of $[(\text{tpy})\text{Ru}^{\text{II}}(\text{tpyPh-DPA})]^{2+}$ (ML) in (2:1 $\text{d}_4\text{-MeOD}:\text{D}_2\text{O}$ v/v) with deuterated MES buffer (0.1M, pH 6) (red) at room temperature and the calculated spectrum (dotted grey) of $[(\text{tpy})\text{Ru}^{\text{II}}(\text{tpyPh-DPA})]^{2+}$ in methanol solution with TD-DFT, MPW1PW91/D95V/LanL2TZ(f).

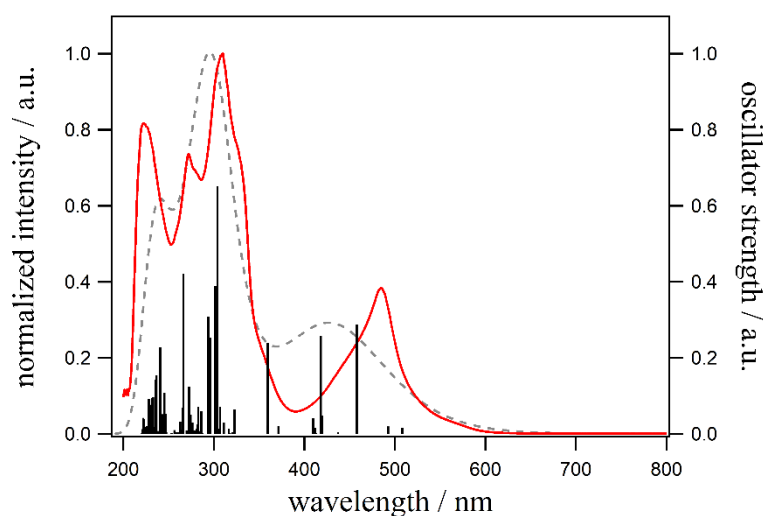


Figure S14. Comparison of UV-Vis absorption spectrum of $[(\text{tpy})\text{Ru}^{\text{II}}(\text{tpyPh-DPA})\text{Lu}^{\text{III}}(\text{H}_2\text{O})_x]^{3+}$ in (2:1 $\text{d}_4\text{-MeOD}:\text{D}_2\text{O}$ v/v) with deuterated MES buffer (0.1M, pH 6) (red) at room temperature and the calculated spectrum (dotted grey) of $[(\text{tpy})\text{Ru}^{\text{II}}(\text{tpyPh-DPA})\text{Lu}^{\text{III}}(\text{H}_2\text{O})_5]^{3+}$ in methanol solution with TD-DFT, MPW1PW91/D95V/LanL2TZ(f) (Ru^{II})/def2-QZVP (Lu^{III}).

Gaussian Model Coordinates

Atomic coordinates of the DFT-optimized $[(\text{tpy})\text{Ru}^{\text{II}}(\text{tpyPh-DPA})]^{2+}$ with MPW1PW91/D95V/LanL2TZ(f) (Ru^{II})/SMD:Methanol.

0 1

C	8.08219500	0.00053100	-0.00034500	H	4.25433600	2.36860500	4.57439200
N	5.33102500	0.00020700	-0.00012700	H	4.90649100	1.26824400	2.43859600
C	7.38682100	-1.08115100	0.55983700	H	1.77771100	2.43309500	-1.26932500
C	7.38647700	1.08205200	-0.56041300	H	2.42532200	4.57587600	-2.35863200
C	5.98691600	1.06208100	-0.54660700	H	4.87247900	5.11861300	-2.61227100
C	5.98725300	-1.06150800	0.54625500	H	6.55902700	3.49296800	-1.77036100
C	5.07613800	2.09070600	-1.07407300	H	7.92736400	1.91284800	-0.99401400
C	3.19111800	3.89651100	-2.00623600	H	7.92796200	-1.91183700	0.99333300
N	3.73169800	1.80873800	-0.93783800	H	6.56011800	-3.49220900	1.77002900
C	5.50220100	3.28043300	-1.67374000	H	4.87407800	-5.11824500	2.61219700
C	4.55343700	4.19432200	-2.14571300	H	2.42675500	-4.57612000	2.35885100
C	2.81909800	2.69661100	-1.39720300	H	1.77847900	-2.43352600	1.26957200
C	5.07679500	-2.09034200	1.07386900	C	-2.89654200	-0.00012000	0.00009100
C	3.19233900	-3.89657600	2.00633500	C	-5.74367800	-0.00007800	0.00005400
C	5.50322700	-3.27994300	1.67352400	C	-3.62152300	1.05483700	0.59196900
N	3.73226900	-1.80870100	0.93780700	C	-3.62153900	-1.05505100	-0.59181100
C	2.81994700	-2.69678400	1.39731700	C	-5.01844400	-1.05781800	-0.58607000
C	4.55474800	-4.19404900	2.14564800	C	-5.01842800	1.05764600	0.58619000
Ru	3.34561400	-0.00002400	0.00000200	H	-3.09737200	1.89042000	1.04345600
C	2.12710200	2.16249000	4.18476500	H	-3.09740100	-1.89063700	-1.04330600
N	2.95406500	0.94124600	1.80765200	H	-5.54357000	-1.88234100	-1.05610500
C	1.18043500	1.69014500	3.26897300	H	-5.54354300	1.88219700	1.05618800
C	3.49002300	2.01631200	3.89329600	N	-10.05423900	0.00002100	-0.00000600
C	3.86453000	1.40100900	2.69740700	C	-9.36215300	-1.16070500	0.06325200
C	1.60892300	1.08335000	2.08398100	C	-10.14694800	-2.46334700	0.13591600
C	0.70138200	0.55323100	1.05293600	C	-7.96018800	-1.19849400	0.06883600
C	-0.69414800	-0.56731000	-1.07215200	C	-7.22614200	-0.00004500	0.00002900
C	-0.69413200	0.56703000	1.07233700	C	-7.96012900	1.19843800	-0.06879400
N	1.36355200	-0.00014500	0.00007800	C	-10.14683400	2.46338800	-0.13593800
C	0.70136700	-0.55352000	-1.05276700	C	-9.36209700	1.16071300	-0.06325200
C	-1.41559200	-0.00013500	0.00009400	H	-7.46582300	-2.15778000	0.14446900
C	1.60889000	-1.08362400	-2.08383600	H	-7.46571500	2.15770000	-0.14442200
C	3.48996100	-2.01659000	-3.89317700	H	9.16547800	0.00065700	-0.00043600
C	1.18038100	-1.69053500	-3.26876000	O	-9.46064000	-3.54250300	0.32625300
N	2.95403500	-0.94140300	-1.80758800	O	-11.42469500	-2.42294200	0.00143200
C	3.86448600	-1.40116800	-2.69735600	O	-11.42459500	2.42302200	-0.00157100
C	2.12703500	-2.16288400	-4.18456600	O	-9.46047100	3.54252600	-0.326
H	-1.21970300	0.99161400	1.91718800				
H	-1.21972700	-0.99189600	-1.91699600				
H	0.12306500	-1.79308900	-3.47657500				
H	1.80568600	-2.63491600	-5.10525600				
H	4.25426300	-2.36888100	-4.57428600				
H	4.90645100	-1.26829900	-2.43861000				
H	0.12312300	1.79260800	3.47685000				
H	1.80576700	2.63442900	5.10550800				

Atomic coordinates of the DFT-optimized $[(\text{tpy})\text{Ru}^{\text{II}}(\text{tpyPh-DPA})\text{Lu}^{\text{III}}(\text{H}_2\text{O})_5]^{3+}$ with MPW1PW91/D95V/LanL2TZ(f) (Ru^{II})/def2-QZVP (Lu^{III})/SMD:Methanol.

3 1				H	-7.76725500	5.28592700	2.27816100
C	-10.99480700	0.01580600	0.01568500	H	-9.45879100	3.61192800	1.55087400
N	-8.24418200	0.00962300	0.00605600	H	-10.83428900	1.98828600	0.88183200
C	-10.30383100	-1.10161200	-0.47568000	H	-10.84921800	-1.95749500	-0.85135000
C	-10.29537200	1.13014700	0.50203600	H	-9.48603900	-3.58381300	-1.53697300
C	-8.89591300	1.10583300	0.48548200	H	-7.80735900	-5.26599600	-2.27554100
C	-8.90419600	-1.08346900	-0.46910100	H	-5.35772300	-4.71629900	-2.06242200
C	-7.98115800	2.16399600	0.94285600	H	-4.70065500	-2.51052100	-1.11539500
C	-6.08996400	4.02286300	1.74964100	C	-0.01823200	-0.00754300	-0.00699600
N	-6.63774200	1.87048200	0.82204700	C	2.82395300	-0.00806700	-0.00939500
C	-8.40296500	3.39105600	1.46492600	C	0.70451500	1.04564800	-0.60419400
C	-7.45118500	4.33213800	1.87309300	C	0.70509100	-1.06123300	0.58861600
C	-5.72215600	2.78462200	1.22002400	C	2.10188300	-1.06674200	0.57846000
C	-7.99743000	-2.14568200	-0.93291800	C	2.10121400	1.05058100	-0.59655500
C	-6.12054400	-4.01331200	-1.75260000	H	0.17769800	1.87728500	-1.05969600
C	-8.42856100	-3.36927600	-1.45546300	H	0.17871000	-1.89261600	1.04510400
N	-6.65185100	-1.85963900	-0.81840300	H	2.62759300	-1.89076800	1.04860800
C	-5.74331500	-2.77805300	-1.22263600	H	2.62620300	1.87439500	-1.06785100
C	-7.48403800	-4.31482200	-1.87006700	N	7.10149300	-0.00582400	-0.00932800
Ru	-6.25782900	0.00413500	0.00148400	C	6.42908300	-1.16626000	-0.11632200
C	-5.04377400	1.90583900	-4.30875400	C	7.31965500	-2.37621300	-0.25091300
N	-5.86859200	0.83075400	-1.86113800	C	5.03510600	-1.21134600	-0.11461600
C	-4.09642500	1.49308200	-3.36523000	C	4.30444000	-0.00742300	-0.00988000
C	-6.40632200	1.77426400	-4.00920700	C	5.03309100	1.19771600	0.09193300
C	-6.77979600	1.23309800	-2.77765600	C	7.31882300	2.36237400	0.20580000
C	-4.52365300	0.95859400	-2.14563400	C	6.42676000	1.15320400	0.09179400
C	-3.61496100	0.49155800	-1.08558100	H	4.53647700	-2.16695100	-0.21641900
C	-2.21806700	-0.51541500	1.09699000	H	4.53371700	2.15331400	0.18996000
C	-2.21913000	0.50523600	-1.10587900	H	-12.07807900	0.01817800	0.01967600
N	-4.27600200	-0.00105000	-0.00167200	O	6.81325500	-3.53284300	-0.35278400
C	-3.61395000	-0.49637500	1.08039300	O	8.59839000	-2.10664000	-0.25308500
C	-1.49959700	-0.00623700	-0.00531900	O	8.59815100	2.08698700	0.17733400
C	-4.52171000	-0.95932600	2.14305900	O	6.82155600	3.52018800	0.31404600
C	-6.40280000	-1.76656200	4.01194600	O	9.03906800	-0.74946800	2.12739800
C	-4.09349600	-1.49630300	3.36120700	O	10.85289500	1.12634900	1.53001100
N	-5.86687900	-0.82490600	1.86261700	O	11.07756300	1.20553100	-1.21228500
C	-6.77730200	-1.22319600	2.78168700	O	11.27271000	-1.44639900	-0.03271700
C	-5.04002100	-1.90473800	4.30743800	O	9.04384100	-0.21860500	-2.25825900
H	-1.68994700	0.88434400	-1.97034900	H	9.36995300	-0.29029200	2.91800100
H	-1.68795100	-0.89626900	1.96014000	H	8.47980900	-1.50733400	2.36901600
H	-3.03656800	-1.59380200	3.57191200	H	11.62239900	0.76683400	2.00321600
H	-4.71872500	-2.32113100	5.25456700	H	10.72815300	2.06870800	1.73575000
H	-7.16730200	-2.07050400	4.71565100	H	11.66299800	1.85175700	-0.78245400
H	-7.81939800	-1.09991500	2.51896900	H	11.31451400	1.09284500	-2.14833700
H	-3.03963900	1.58535200	-3.57903900	H	11.15283500	-2.40962100	0.03340600
H	-4.72329200	2.32041200	-5.25695800	H	12.20168700	-1.22615800	-0.21561400
H	-7.17142300	2.08167400	-4.71075600	H	8.52063500	-0.96054200	-2.60798300
H	-7.82167700	1.11486800	-2.51175600	H	9.10741100	0.49445300	-2.91766900
H	-4.68152900	2.51114400	1.10795400	Lu	9.49543000	0.00600900	-0.002383
H	-5.32174200	4.72221100	2.05430900				

VI. Photophysical Data

All steady state and emission measurements were carried out using 1 or 0.3 cm quartz cuvettes using (2:1 d_4 -MeOD: D_2O v/v) as the solvent. The UV-Vis absorption measurements were carried out using an Agilent Cary 60 UV-Vis spectrometer and the obtained spectra were recorded using Cary WinUV Scan Application (Version 5.0.0.999). Emission measurements were performed using Horiba JY FluoroLog-311 spectrofluorimeter and the spectra were obtained using the FluorEssence software. Femtosecond transient absorption studies (HELIOS) were undertaken using an amplified laser (Spitfire ACE, Spectra Physics) as the excitation source, delivering ca. 100 fs 800 nm laser pulses at a 1 kHz repetition rate. Approximately 0.1 mJ of this output was focused onto a CaF_2 crystal to generate a white light continuum probe pulse from ca. 350 nm to 700 nm. The remainder of the output was coupled to an OPA system (TOPAS PRIME, Light Conversion) delivering femtosecond tuneable excitation pulses at 485 nm. The pump pulse polarisation was set to magic angle with respect to the probe. Absorbance of the samples was ca. 0.5 over the 2 mm path length cell used, and samples were continuously stirred mechanically. The instrument response function (IRF) for this setup is approximately 250 fs. The resulting transient data were analysed globally using commercially available software (Igor, Version 6.1.2.1, Wavemetrics).

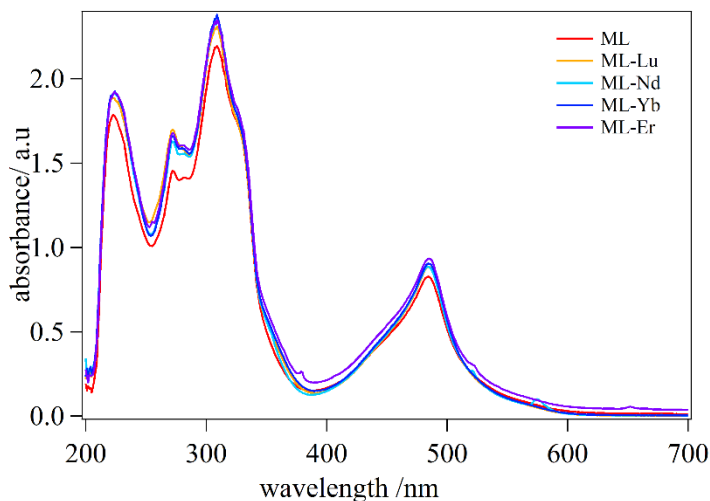


Figure S15: UV-Vis spectra of 1:1 ML-Ln^{III} complexes where ML = [(tpy)Ru^{II}(tpyPh-DPA)] and Ln = Lu, Nd, Yb or Er in (2:1 d_4 -MeOD: D_2O v/v) with deuterated MES buffer (0.1M, pD 6.4).

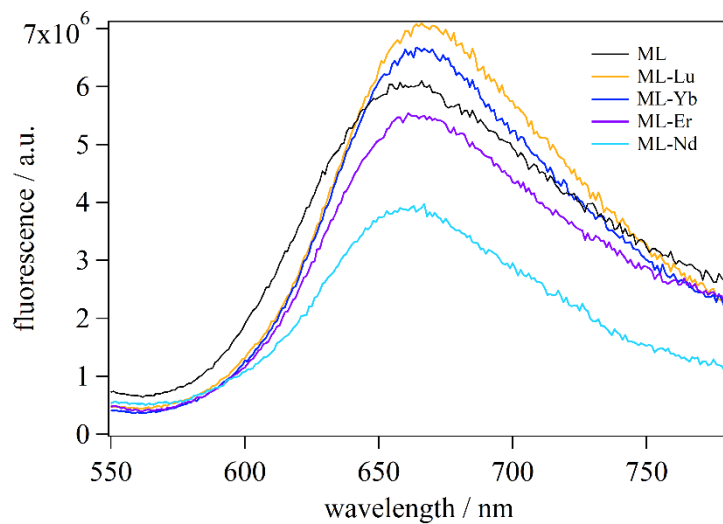


Figure S16: Emission spectra of ML and 1:1 ML-Ln^{III} complexes upon 485 nm excitation where ML = [(tpy)Ru^{II}(tpyPh-DPA)] and Ln = Lu, Nd, Yb or Er in (2:1 d₄-MeOD: D₂O v/v) with deuterated MES buffer (0.1M, pD 6.4).

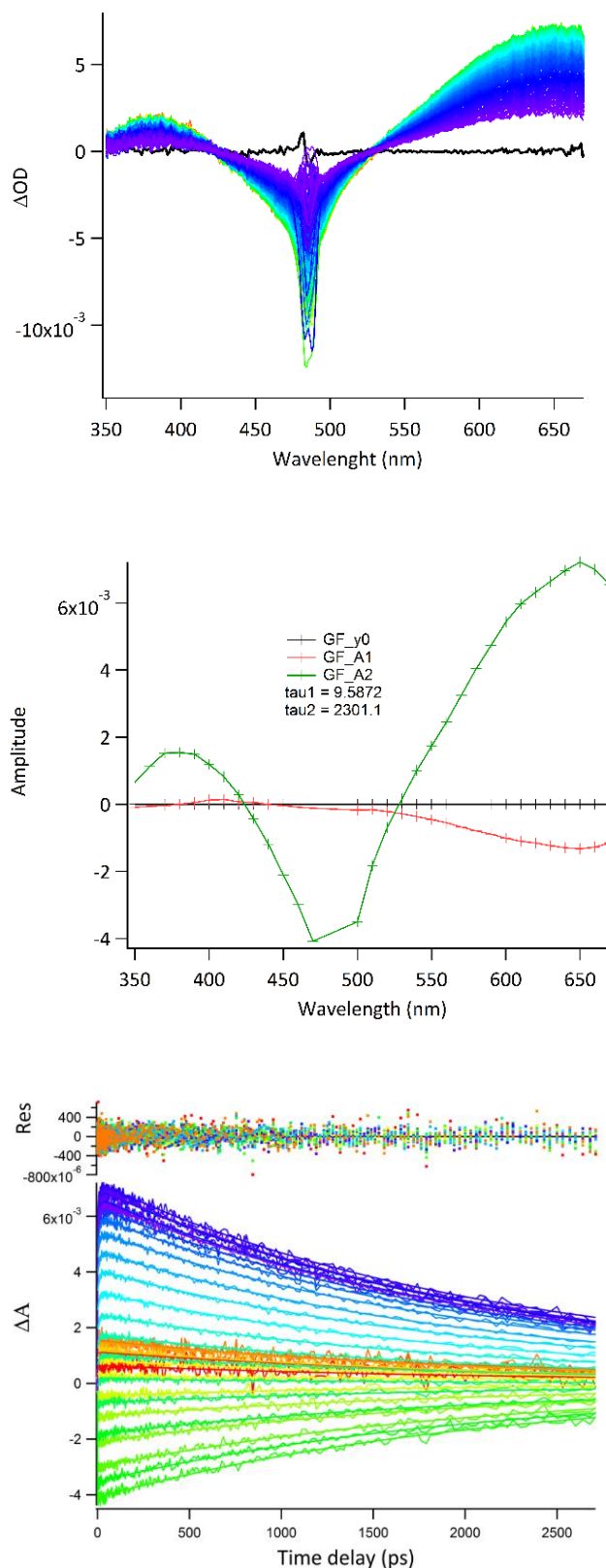


Figure S17. TA spectra (top), Decay Associated Difference Spectra (middle) and a globally fit kinetic plot (bottom) for [(tpy)Ru^{II}(tpyPh-DPA)] in (2:1 d₄-MeOD: D₂O v/v) with deuterated MES buffer (0.1M, pD 6.4).

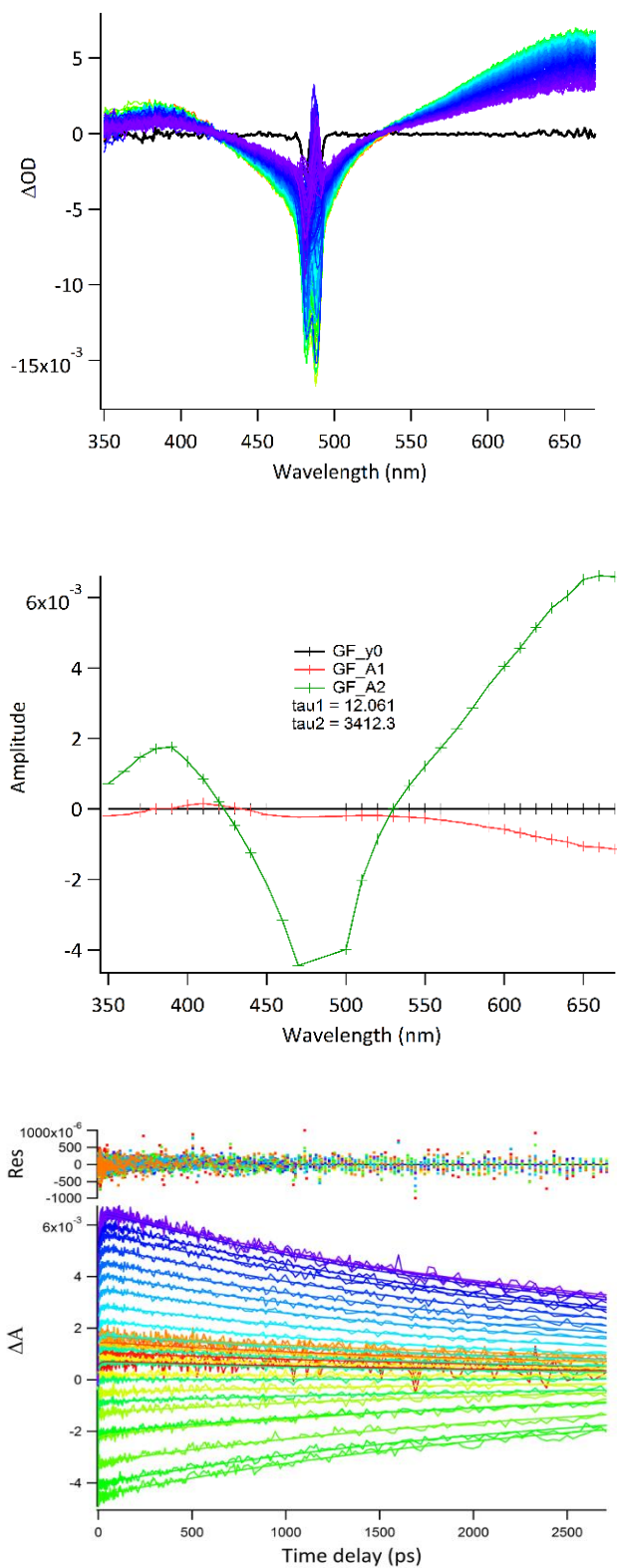


Figure S18. TA spectra (top), Decay Associated Difference Spectra (middle) and a globally fit kinetic plot (bottom) for $[(\text{tpy})\text{Ru}^{\text{II}}(\text{tpyPh-DPA})\text{Lu}^{\text{III}}(\text{H}_2\text{O})_x]^{3+}$ in (2:1 d_4 -MeOD: D_2O v/v) with deuterated MES buffer (0.1M, pD 6.4).

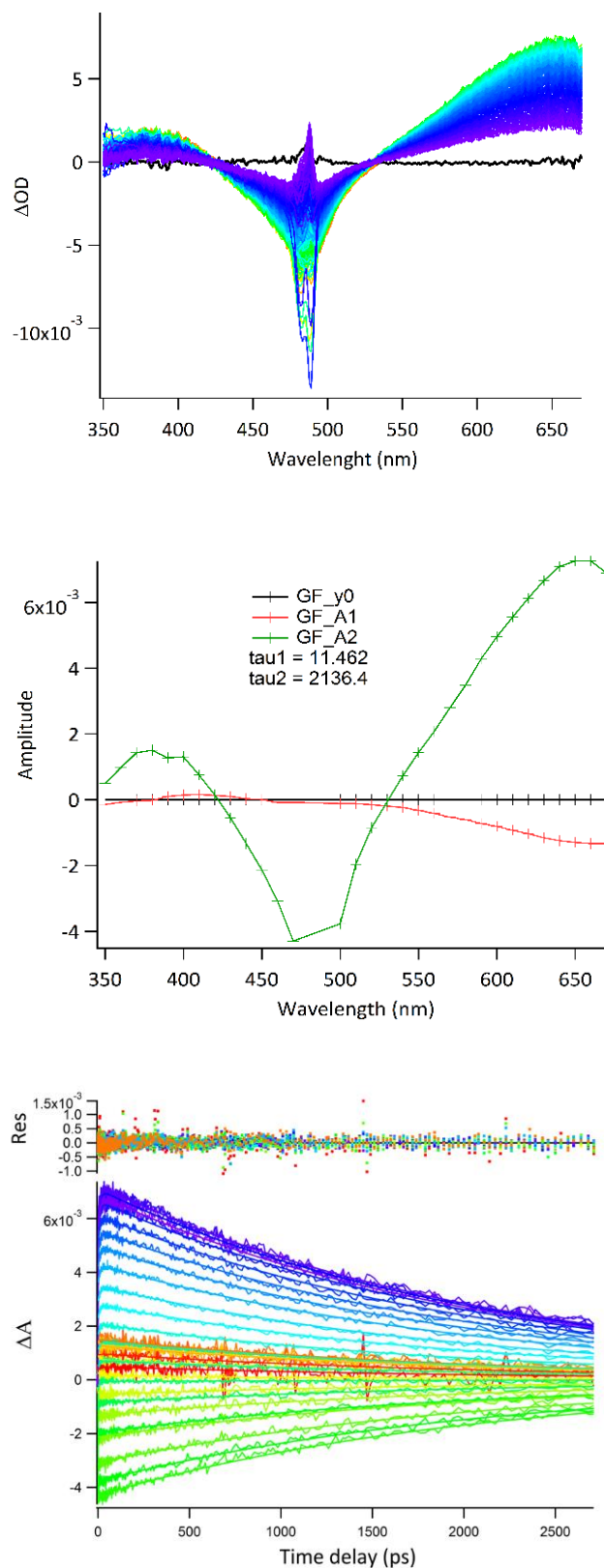


Figure S19. TA spectra (top), Decay Associated Difference Spectra (middle) and a globally fit kinetic plot (bottom) for $[(\text{tpy})\text{Ru}^{\text{II}}(\text{tpyPh-DPA})\text{Nd}^{\text{III}}(\text{H}_2\text{O})_x]^{3+}$ in (2:1 $\text{d}_4\text{-MeOD} : \text{D}_2\text{O}$ v/v) with deuterated MES buffer (0.1M, pD 6.4).

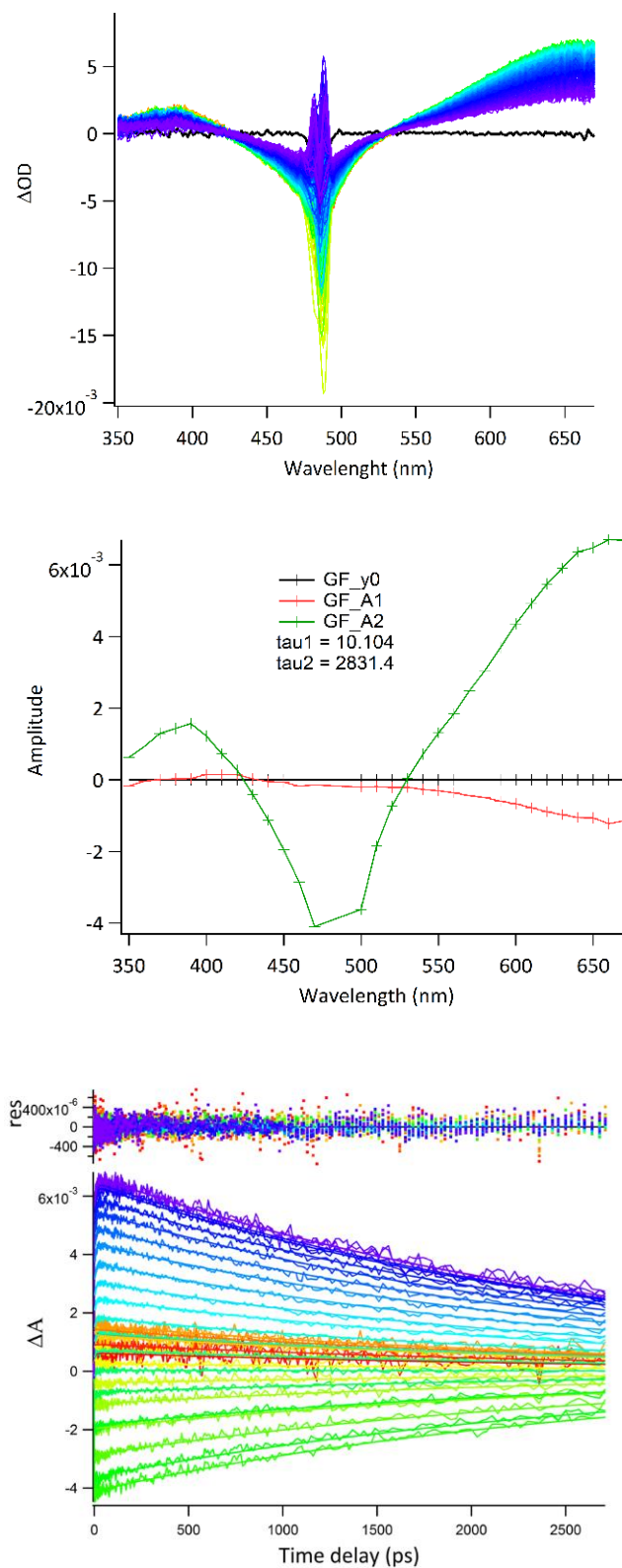


Figure S20:: TA spectra (top), Decay Associated Difference Spectra (middle) and a globally fit kinetic plot (bottom) for $[(\text{tpy})\text{Ru}^{\text{II}}(\text{tpyPh-DPA})\text{Er}^{\text{III}}(\text{H}_2\text{O})_x]^{3+}$ in (2:1 $\text{d}_4\text{-MeOD}:\text{D}_2\text{O}$ v/v) with deuterated MES buffer (0.1M, pD 6.4).

VII. References

1. R. A. Tigaa, G. J. Lucas and A. de Bettencourt-Dias, *Inorg. Chem.*, 2017, **56**, 3260-3268.
2. O. K. Rasheed, C. Bawn, D. Davies, J. Raftery, I. Vitorica-Yrzebal, R. Pritchard, H. Zhou and P. Quayle, *Eur. J. Org. Chem.*, 2017, **2017**, 5252-5261.
3. O. K. Rasheed, J. J. W. McDouall, C. A. Muryn, J. Raftery, I. J. Vitorica-Yrezabal and P. Quayle, *Dalton Trans.*, 2017, **46**, 5229-5239.
4. S. Katagiri, R. Sakamoto, H. Maeda, Y. Nishimori, T. Kurita and H. Nishihara, *Chem. Eur. J.*, 2013, **19**, 5088-5096.
5. C. J. Aspley and J. A. Gareth Williams, *New J. Chem.*, 2001, **25**, 1136-1147.
6. F. Barigelletti, L. Flamigni, V. Balzani, J.-P. Collin, J.-P. Sauvage, A. Sour, E. C. Constable and A. M. W. C. Thompson, *J. Am. Chem. Soc.*, 1994, **116**, 7692-7699.
7. C. Chakraborty, U. Rana, R. K. Pandey, S. Moriyama and M. Higuchi, *ACS Appl. Mater. Interfaces*, 2017, **9**, 13406-13414.
8. A. Krężel and W. Bal, *J. Inorg. Biochem.*, 2004, **98**, 161-166.
9. C. P. Agilent and P. CrysAlis, 2014.
10. O. V. Dolomanov, L. J. Bourhis, R. J. Gildea, J. A. Howard and H. Puschmann, *J. Appl. Crystallogr.*, 2009, **42**, 339-341.
11. G. M. Sheldrick, *Acta Crystallogr. A*, 2015, **71**, 3-8.
12. G. Sheldrick, *Acta Crystallogr. A*, 2008, **64**, 112-122.
13. M. J. Frisch, G. W. Trucks, H. B. Schlegel, G. E. Scuseria, M. A. Robb, J. R. Cheeseman, G. Scalmani, V. Barone, G. A. Petersson, H. Nakatsuji, X. Li, M. Caricato, A. V. Marenich, J. Bloino, B. G. Janesko, R. Gomperts, B. Mennucci, H. P. Hratchian, J. V. Ortiz, A. F. Izmaylov, J. L. Sonnenberg, Williams, F. Ding, F. Lipparini, F. Egidi, J. Goings, B. Peng, A. Petrone, T. Henderson, D. Ranasinghe, V. G. Zakrzewski, J. Gao, N. Rega, G. Zheng, W. Liang, M. Hada, M. Ehara, K. Toyota, R. Fukuda, J. Hasegawa, M. Ishida, T. Nakajima, Y. Honda, O. Kitao, H. Nakai, T. Vreven, K. Throssell, J. A. Montgomery Jr., J. E. Peralta, F. Ogliaro, M. J. Bearpark, J. J. Heyd, E. N. Brothers, K. N. Kudin, V. N. Staroverov, T. A. Keith, R. Kobayashi, J. Normand, K. Raghavachari, A. P. Rendell, J. C. Burant, S. S. Iyengar, J. Tomasi, M. Cossi, J. M. Millam, M. Klene, C. Adamo, R. Cammi, J. W. Ochterski, R. L. Martin, K. Morokuma, O. Farkas, J. B. Foresman and D. J. Fox, *Journal*, 2016.
14. C. Adamo and V. Barone, *J. Chem. Phys.*, 1998, **108**, 664-675.
15. T. H. Dunning Jr and P. J. Hay, 1976.
16. A. W. Ehlers, M. Böhme, S. Dapprich, A. Gobbi, A. Höllwarth, V. Jonas, K. F. Köhler, R. Stegmann, A. Veldkamp and G. Frenking, *Chem. Phys. Lett.*, 1993, **208**, 111-114.
17. P. J. Hay and W. R. Wadt, *J. Chem. Phys.*, 1985, **82**, 299-310.
18. L. E. Roy, P. J. Hay and R. L. Martin, *J. Chem. Theory Comput.*, 2008, **4**, 1029-1031.
19. R. Gulde, P. Pollak and F. Weigend, *J. Chem. Theory Comput.*, 2012, **8**, 4062-4068.
20. A. V. Marenich, C. J. Cramer and D. G. Truhlar, *J. Phys. Chem. B*, 2009, **113**, 6378-6396.